iScience

CellPress
OPEN ACCESS

Article

The relativity of reaching: Motion of the touched surface alters the trajectory of hand movements

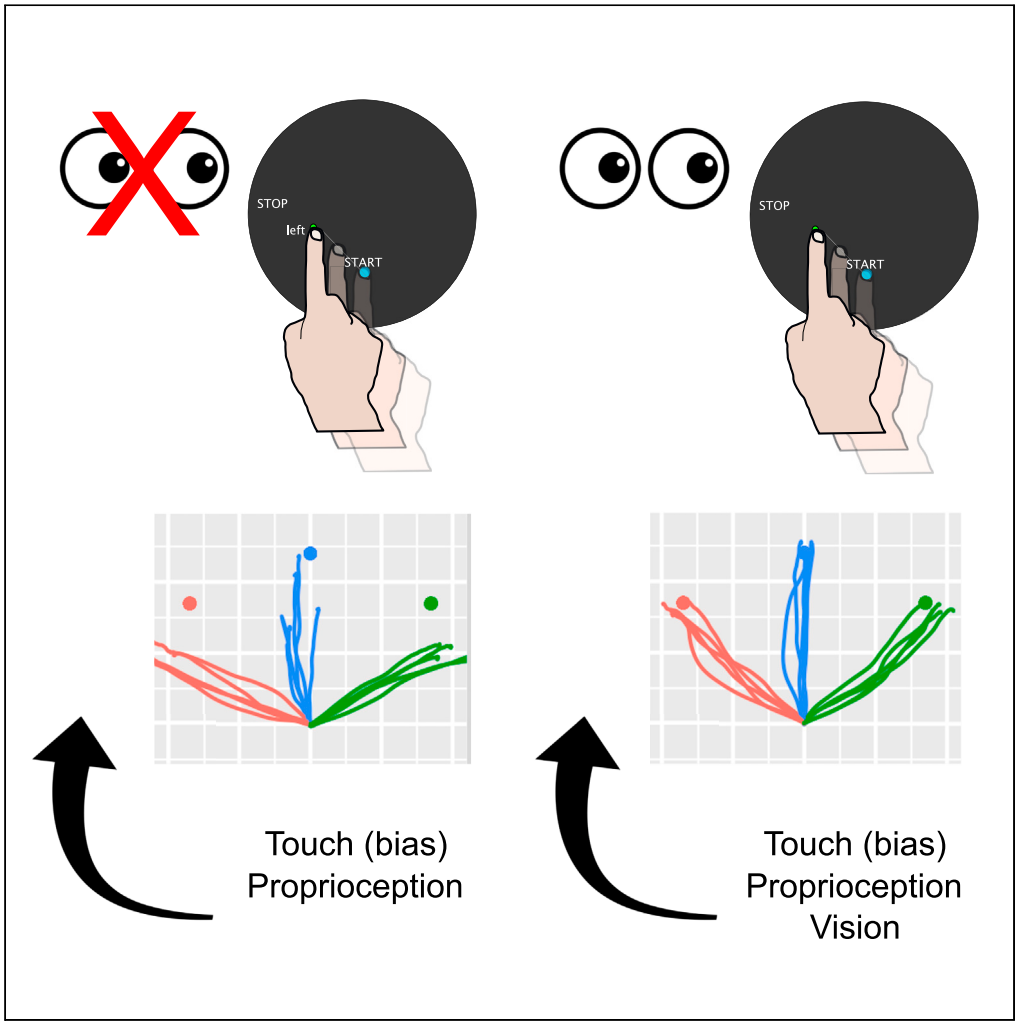

Colleen P. Ryan, Simone Ciotti, Priscilla Balestrucci, Antonio Bicchi, Francesco Lacquaniti, Matteo Bianchi, Alessandro Moscatelli

lacquaniti@med.uniroma2.it (F.L.)
a.moscatelli@hsantalucia.it (A.M.)

Highlights

Objects are generally stationary and humans use this assumption in sensorimotor tasks

Violation of this assumption during a reaching task produced systematic motor errors

Tactile sensitivity and visual feedback modulate the motor errors

Errors can be explained by model assuming integration of somatosensory and visual cues

Ryan et al., iScience 27, 109871
June 21, 2024
https://doi.org/10.1016/j.isci.2024.109871

iScience

CellPress
OPEN ACCESS

Article

The relativity of reaching: Motion of the touched surface alters the trajectory of hand movements

Colleen P. Ryan,[1,2,5] Simone Ciotti,[2,3,5] Priscilla Balestrucci,[2] Antonio Bicchi,[3,4] Francesco Lacquaniti,[1,2,*] Matteo Bianchi,[3] and Alessandro Moscatelli[1,2,6,*]

SUMMARY

For dexterous control of the hand, humans integrate sensory information and prior knowledge regarding their bodies and the world. We studied the role of touch in hand motor control by challenging a fundamental prior assumption—that self-motion of inanimate objects is unlikely upon contact. In a reaching task, participants slid their fingertips across a robotic interface, with their hand hidden from sight. Unbeknownst to the participants, the robotic interface remained static, followed hand movement, or moved in opposition to it. We considered two hypotheses. Either participants were able to account for surface motion or, if the stationarity assumption held, they would integrate the biased tactile cues and proprioception. Motor errors consistent with the latter hypothesis were observed. The role of visual feedback, tactile sensitivity, and friction was also investigated. Our study carries profound implications for human-machine collaboration in a world where objects may no longer conform to the stationarity assumption.

INTRODUCTION

Sliding movements to follow a path or to reach for a target on a planar surface are common in our daily life. For example, we perform a sequence of short sliding movements to unlock our smartphone, when reaching toward the computer mouse on our desk, or when we follow a contour of an object to know its shape.[1,2]

Classical studies in neuroscience shed light on fundamental properties of reaching movements in 2D, in both humans and in non-human primates.[3,4] Precise sensory feedback is crucial to achieve the high level of dexterity characterizing reaching movements in humans.[3,5,6] The somatosensory and the visual systems inform our brain about the position and movement of our hand and the location of the target.[7–10] During reaching tasks, the brain integrates proprioception and vision in an optimal fashion, meaning that the relative weight of each sensory channel depends on its reliability.[7,8] In classical studies on 2D reaching, often the movement was constrained on a plane by means of a handheld manipulandum[11–14] or by an exoskeleton[15] recording the reaching trajectories and occasionally applying external forces. In the tasks above, the interfaces prevented slip motion from occurring. Instead, as anticipated above, sliding our fingertips on the surface of an object to interact with it or to perceive its properties are more common experiences in daily life. Recent studies investigated the integration between slip motion and proprioception in reaching tasks[9,10,16,17] and in other tasks requiring hand motion.[18–21] It was shown that it is possible to decouple touch and proprioception by changing the orientation of a texture with raised lines.[10] In this study, participants slid their fingertip on a plate with ridges to move toward a target without any visual feedback on hand location. Tactile motion estimates were biased by changing the ridge orientation, as accounted for by the tactile flow model,[22] and this induced a systematic deviation in hand trajectories. These results were confirmed in a later study where the ridged plate rotated during the reaching task.[23] In another study,[9] participants were requested to contact the far end of a rod with their right hand, while the occasional rotation of the rod was measured by their left hand contacting it at its near end. Spatial information about a sudden change in tool orientation, provided by tactile cues on one hand, evoked a rapid correction of the movement of the other hand.

Albeit tools can occasionally move, as in the task described above, most of the objects we interact with are usually stationary. Observers assume *a priori* that, statistically speaking, inanimate objects are generally at rest with respect to their body. Accordingly, a mathematical model including a prior for object stationarity can account for different aspects of human perception.[24–27] According to this model, a deformation on the skin is more likely to be interpreted as our limbs moving against a static object rather than a moving object impacting on our static limbs, that is, humans are more likely to move than inanimate things in the environment. Because of this prior belief, observers are fairly inaccurate in combining surface and hand motion.[27,28] For example, they perceive a surface that moves away from them as stationary while sliding their hand on it.[27] The human brain has adapted to a world where inanimate objects we interact with are substantially static. However,

[1]Department of Systems Medicine and Centre of Space Biomedicine, University of Rome Tor Vergata, 00133 Rome, Italy
[2]Laboratory of Neuromotor Physiology, Santa Lucia Foundation IRCCS, 00179 Rome, Italy
[3]Research Centre E. Piaggio and Department of Information Engineering, University of Pisa, 56122 Pisa, Italy
[4]Istituto Italiano di Tecnologia, 16163 Genova, Italy
[5]These authors contributed equally
[6]Lead contact
*Correspondence: lacquaniti@med.uniroma2.it (F.L.), a.moscatelli@hsantalucia.it (A.M.)
https://doi.org/10.1016/j.isci.2024.109871

Table 1. The three values of gain for the x and the y axis of motion

Gain	Plate motion
−0.7	opposite to the hand
0	static
0.7	following the hand

non-negligible exceptions also exist. The emergence of mechatronic devices such as collaborative robots and interfaces for extended reality gives rise to a world that is continuously more dynamic. This raises the question of how human movements would change if the objects around us would also start moving, thereby violating the stationarity assumption.

Here, to answer this question, we investigated how the reaching trajectory would change if the touched surface also moved. Participants slid the index fingertip on a plate moved by a robotic interface[29] and performed a reaching movement toward a virtual target, with their hand hidden from view. They were requested to keep motion speed similar across trials. Unbeknownst to the participant, the position of the plate was continuously updated depending on the position of the hand multiplied by a gain factor that changed across trials. By varying the gain factor, it was possible to decouple local slip motion from hand motion. Depending on the gain, the plate was either stationary (consistent with the static assumption by the observers), following the hand or moving opposite to it (Table 1). The three conditions were implemented independently along either actuated axis of the interface (Figures 1A and 1B and detailed in our previous publication[29]). To reduce friction, the surface of the contact plate was covered with fine textured Teflon material and was lubricated prior to the experiment (Figure 1C). Videos of the device moving in the different conditions are available on Zenodo (Zenodo: https://doi.org/10.5281/zenodo.6124172). The procedure is illustrated in Figures 2A and 2B, and detailed in the STAR Methods section.

We predicted the response to the task by assuming the optimal integration between proprioception and touch.[10] Because of the violation of the stationarity assumption in the moving conditions, we expected that participants would be deceived by tactile motion estimates resulting in systematic errors in reaching movement. In two further experiments we tested the modulation of the effect when the relevance of tactile motion was decreased, either by including visual feedback or by reducing tactile sensitivity. Since vision is of primary importance in the control of reaching movement,[7,8] we expect that the biasing effect of tactile motion would be reduced if we provide participants with accurate visual feedback. This further prediction was tested in a second experiment including visual feedback on hand motion. In a third experiment, we investigated the role of tactile sensitivity and frictional forces on the motor errors.

RESULTS

Model and predictions

According to previous studies, humans assume that the objects they interact with do not usually move. If this assumption holds, when sliding the fingertip on a surface proprioceptive and tactile signals provide redundant cues about hand velocity. Then, the two sensory measurements can be optimally integrated and the perceived velocity of the hand $\widehat{h}_i$ would be a weighted sum of proprioception and touch (in the absence of vision). For each axis of motion i in the x-y plane, the integrated velocity can be accounted for by an ideal observer model detailed in the following (Equation 1).

$$\widehat{h}_i = w_k \widehat{h}_{ik} + w_c \widehat{h}_{ic} \quad \text{(Equation 1)}$$

Where $\widehat{h}_{ik}$ are the velocity measurements from kinesthetic signals (i.e., proprioception), $\widehat{h}_{ic}$ are those from cutaneous signals (i.e., touch from slip motion cues). The terms w_k, w_c are the corresponding weight terms which represent the relative contribution of each sensory information, with their sum equal to one. We hypothesize that the sensorimotor system would continue to rely on computations similar to the one expressed in Equation 1 even when the assumption of stationarity is violated because of movement of the object. If so, a movement of the plate either following or opposite to the hand (Table 1) would produce a systematic error in reaching movements. The predictions of the observer model are illustrated in Figure 3 and detailed in the Appendix. In negative gain conditions, the plate moves opposite to the hand movement and the velocity of slip motion measured by touch is faster than the actual hand motion (Figures 3A and 3D). Therefore, participants would overestimate the speed of hand motion, compensate by moving slower, and stop before the target. Vice versa, participants would move faster and stop after the target in positive gain conditions.

Based on the predicted hand velocity, the motion path for the three different targets (to the left, center, and right; Figure 3B) and the nine gain combinations (three gain values along the x axis times three gain values along the y axis) were derived. To this aim, we assumed that participants attempted to move with the same velocity profile across trials, as requested by the task.

The gain combination along the two axes would affect both path length and motion angle (Figure 3B). As illustrated in the figure, predicted hand velocity and path length can be approximated as a linear function of the gain (Figures 3C and 3D).

Finally, we predicted the effect of the gain on the final motion angle (as detailed in the STAR Methods section, paragraph on predictions of the vector model). According to the model, the desired angle $\bar{\theta}$ (i.e., the angle between the starting position and the virtual targets) and the observed motion angle θ (the angle to the final position of the finger) are related by the following equation (Equation 2).

$$\cot(\bar{\theta}) = \cot(\theta)\frac{1 - w_c\gamma_x}{1 - w_c\gamma_y} \quad \text{(Equation 2)}$$

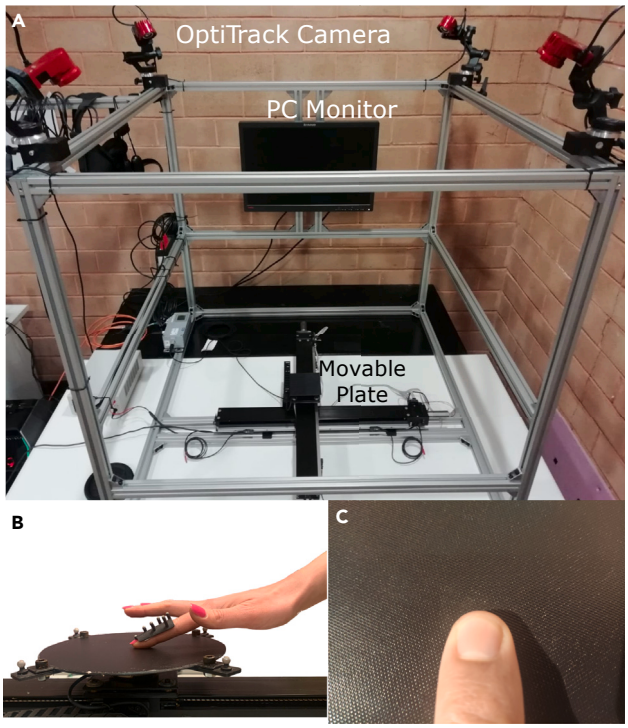

Figure 1. The experimental setup used in Exp 1-3

(A) Aerial view of the HaptiTrack device.

(B) The finger of a participant in contact with the movable plate. Markers are attached on a rigid body on the right index finger for tracking.

(C) The surface of the plate was covered with fine textured Teflon material and was lubricated prior to the experiment.

With w_c being the cutaneous weight term (Equation 1) and the two gain values γ_y and γ_x depending on the experimental condition. It follows that, for a given pair γ_y, γ_x, the cotangent of the observed motion angle is a linear function of the desired motion angle (Equation 3):

$$\cot(\theta) = \cot(\overline{\theta})\beta(w_c, \gamma_x, \gamma_y) \quad \text{(Equation 3)}$$

By fitting Equation 3 to the data, it is possible to estimate the cutaneous weight w_c. In the second experiment, participants were also provided with visual feedback on the velocity of the hand and its position with respect to the target. Therefore, it is possible to rewrite Equation 1 as:

$$\widehat{h}_i = w_k \widehat{h}_{ik} + w_c \widehat{h}_{ic} + w_v \widehat{h}_{iv} \quad \text{(Equation 4)}$$

where $w_v \widehat{h}_{iv}$ represents the contribution of vision to the integrated estimate. Because of the primary importance of vision in the control of reaching movements, we expect that the biasing effect of tactile motion would be smaller in this second experiment. This can be measured by comparing the value of w_c between the two experiments.

In the third experiment, we considered the role of tactile sensitivity and shear forces in the determination of the motor response to changes in gain. In order to manipulate tactile sensitivity, we asked participants to perform the reaching task while wearing a rigid thimble that covered their fingertip. To modulate shear forces, we asked participants to perform the task with their bare fingertip and lubricated the contact plate with different lubricants (i.e., oil or gel). We expected a smaller effect of gain on motor error when wearing the thimble as compared to the bare-fingertip condition, due to the reduced reliability of the tactile channel in the former. Accordingly, the value of w_c is expected to be smaller in the condition with a thimble as compared to the two bare-fingertip conditions. The optimal model described above does not account for the effect of shear forces. However, the values of shear forces were overall small and the movement was not constrained in time, thus allowing for online corrections. Therefore, we expected small or negligible differences in the motor response across lubricants. It is to note that the two factors of sensitivity and shear force cannot be neatly decoupled across experimental conditions, due to the nature of the mechanical stimuli involved.

Experiment 1: Slip motion and reaching movements

Hand velocity

Figures 4A and 4B illustrates the velocity profiles in a representative participant. In accordance with our predictions, the peak speed was lower when the gain was negative (left panel; gain −0.7) and higher during positive gain (right panel; gain 0.7). The linear relationship between

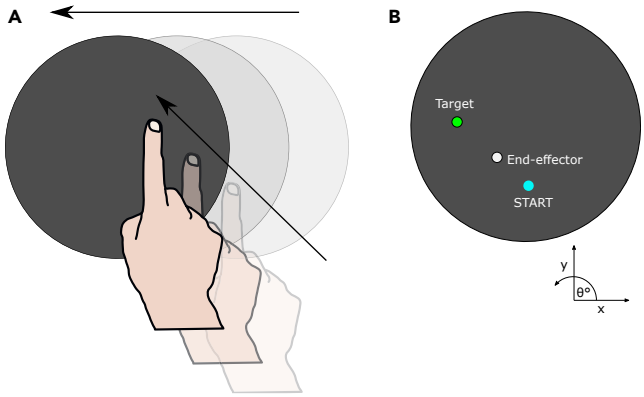

Figure 2. Experimental task and stimuli

(A) Illustration of plate and hand motion. Using this device it is possible to update the position of the plate to separate hand motion and slip motion.

(B) The starting position and the target were displayed on a PC monitor. An exemplary trial illustrating a reaching movement toward the left target. In Experiment 1, the dot indicating the fingertip (end-effector) disappeared at the onset of the trial. The target (green dot) was located at 60 mm from the starting position of the fingertip. The target was located in one of three different positions (left, center, right). The trial was complete when either the participant lifted the finger from the plate or the displacement of the fingertip exceeded 90 mm from the starting position. The coordinate system was centered on the starting position and was oriented as indicated in the sketch in the bottom left corner of the figure.

velocity and gain is shown in Figure 4C. Using linear mixed models (LMMs), for each axis of motion the linear relationship between the peak speed and the gain was tested across all participants. The effect of gain along the x axis was statistically significant on both left (Estimate = −0.28, *p*-value <0.001) and right target (Estimate = 0.39, *p*-value <0.001) with respect to the central target. For reaching movement toward the central target the gain did not produce any effect because there was no displacement along the x axis for this target (Estimate = −0.027, *p*-value = 0.68). The effect of gain on the y axis was statistically significant for all the three targets (Estimate = 0.23, *p*-value = 0.003). This is in accordance with the prediction of our model (Figure 3D). The predicted slope of the LMMs is illustrated for each participant and for the whole group (N = 17) in Figures S7 and S8, for the x and the y axis, respectively.

Motion path and path length

Figures 5A illustrates the motion paths of a representative participant across different targets (left, center, and right) and across the nine possible combinations on x and y gain. Positive and negative values along the x axis are for the leftward and rightward movements, with the origin of the coordinate system corresponding to the starting position. Since the task only required forward movements, values along the y axis are always positive. As evident from the figure, motion paths were different depending on gain conditions. For example, a positive gain along the x or the y axis produced an overly long path along that axis as compared to a negative gain. The motion angle depended on the combination of the x and y gain, with the angle formed by the left and the right path being widest in the panel at the top right corner (i.e., the pattern similar to blossomed flower; $\gamma_y = -0.7, \gamma_x = 0.7$) and narrowest in the panel at the bottom left corner (the pattern similar to a flower bud; $\gamma_y = 0.7, \gamma_x = -0.7$). Notably, this is in accordance with the prediction of the model (Figure 3B).

We tested the hypothesis of a linear relationship between the final position of the fingertip and the gain, for each of the two axes of motion. The model fit is illustrated for a representative participant in Figure 5B and it was extended to all participants by means of an LMM. In accordance with the weighted average model, along the x axis the slope of the linear regression was zero for the central target (Estimate = −0.71, *p*-value = 0.47), positive for the right target (Estimate diff. = 13.85, *p*-value <0.001), negative for the left target (Estimate diff. = −11.44, *p*-value <0.001). Along the y axis the slope was always positive (Estimate = 8.0, *p*-value <0.001). There was no significant interaction between gain and right target (Estimate = −1.13, *p*-value = 0.34), and gain and left target (Estimate = −0.50, *p*-value = 0.68). The predicted slope of the LMM is illustrated for each participant and for the whole group (N = 17) in Figures S9 and S10, for the x and the y axis, respectively.

Motion angle

For each trial we computed the cotangent of the actual motion angle, θ, and of the angle between the starting position and the visual target (the desired angle, $\overline{\theta}$). As detailed in the STAR Methods section, the weighted average model predicted a nonlinear relationship between the desired angle, the actual motion angle and the gain (Equation 3). Next, we fit the nonlinear model to the data, with the weight of tactile channel w_c being the single free parameter. The model provided a good fit to the data, as illustrated in Figure 5C in a representative participant. For each fixed value of gain, the model predicted a linear relationship between $\cot(\theta)$ and $\cot(\overline{\theta})$ with the slope of the linear relationship depending on the x and y gain values, and of the free parameter w_c. The estimated values of w_c across participants were equal to 0.45 ± 0.20 (Mean $\pm$ Standard Deviation).

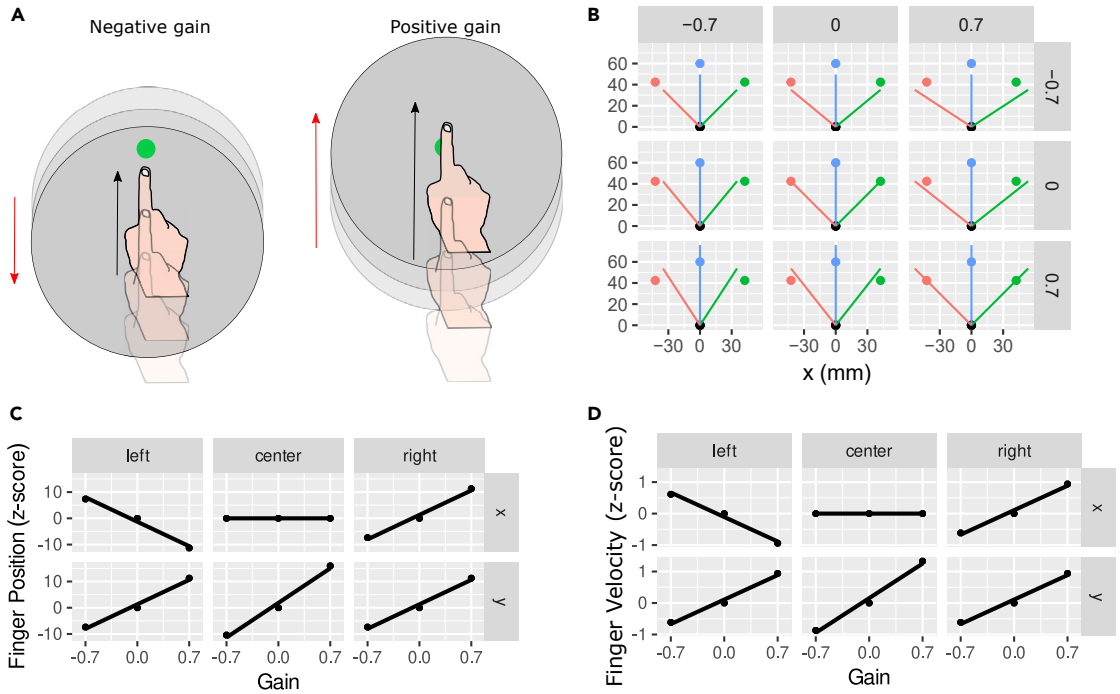

Figure 3. Illustration of model predictions

(A) The left sketch shows an example of negative gain on y axis. The hand velocity decreases (black arrow) and the participant stops before the target (illustrated in green) which leads to a shorter path length. Vice versa for the positive gain shown in the sketch on the right.

(B) From the model we simulated the response of an ideal observer by setting the cutaneous weight: w_c = 0.3. The figure represents the motion paths along the x and y axis for different combinations of gain and target. The left, center and right target are shown in the color red, blue and green respectively.

(C) Predicted final position as a function of the gain values. Predictions for the x and the y axis are illustrated in the top and in the bottom panel, respectively. Raw data were simulated from the model in appendix and fit with linear regression in the scatterplot.

(D) Predicted motion velocity as a function of the gain values. Predictions for the x and the y axis are illustrated in the top and in the bottom panel, respectively.

Analysis of contact forces

Results for the anlaysis of contact forces are illustrated in Figures 6 and 7. The normal force (z axis) was less than the threshold of 2 N, as requested by the task (the mean value ranged from 0.9 to 1.1 N across the different conditions). The texture surface of the device (Figure 1C) was lubricated to reduce the mechanical perturbation by the moving plate. We analyzed tangential forces to verify that the mechanical perturbation was small. Figure 6 illustrates the average profile of shear force over time in the nine gain conditions. The distribution of tangential force (x- and y axis) across all participants is shown in Figure 7. Because of the lubricant, values of tangential forces were overall small. Across conditions, the mean of peak force ranged from 0.001 N to 0.39 N for the x axis and from 0.006 N to 0.39 N for the y axis. Using a linear mixed model, we studied the relationship between the tangential force peak, tactile slip velocity and load force. There was a significant association between the tactile slip velocity and tangential force, such that the faster the slip motion, the higher the module of the force (x axis, Estimate = 0.0008, $p < 0.001$; y axis, Estimate = 0.0004, $p < 0.001$). Because of that, values of shear forces were higher for the negative gain condition, where the plate moved opposite to the hand, and lower for the positive gain condition (Figures 6 and S1). The tangential force was also significantly associated with the load force (x axis: Estimate = 0.09, $p < 001$; y axis: Estimate = 0.17, $p < 001$).

We ran further analyses to disentangle the effect of shear force and gain on hand trajectory (see details in supplemental information). For all gain conditions we selected a subset of data in which the peak value of shear force was less than a fixed threshold. The threshold values were equal to 0.25 N and 0.21 N for the x and the y axis of motion respectively. In this subset of data (low force subset) the values of shear force were homogeneous across gain conditions (Figure S1; Tables S1 and S2). We used LMM to test if the shear forces were the same across the three gain values in the subset of data. In the x axis, the difference in shear force was not statistically significant between positive and zero gain conditions ($p = 0.64$) and between negative and zero gain conditions ($p = 0.84$). In the y axis, the difference in shear force was not statistically significant between positive and zero gain conditions ($p = 0.77$) whereas it was statistically significant between negative and zero gain conditions ($p < 0.001$), although the difference was numerically small (average difference of 0.01 N).

Then, as we did for the full dataset, we evaluated the effect of x and y gain on the reaching movement in the low force subset. By means of LMM, which are robust to unbalanced experimental designs,[30] we tested the hypothesis of a linear relationship between the motion velocity and the gain values. The analyses of the subset of data confirmed the results of the analysis of the full dataset. Specifically, also in this subset of data, the velocity of hand motion was significantly affected by the gain in both axes of motion (Figures S2–S4; Tables S3 and S4). The two terms

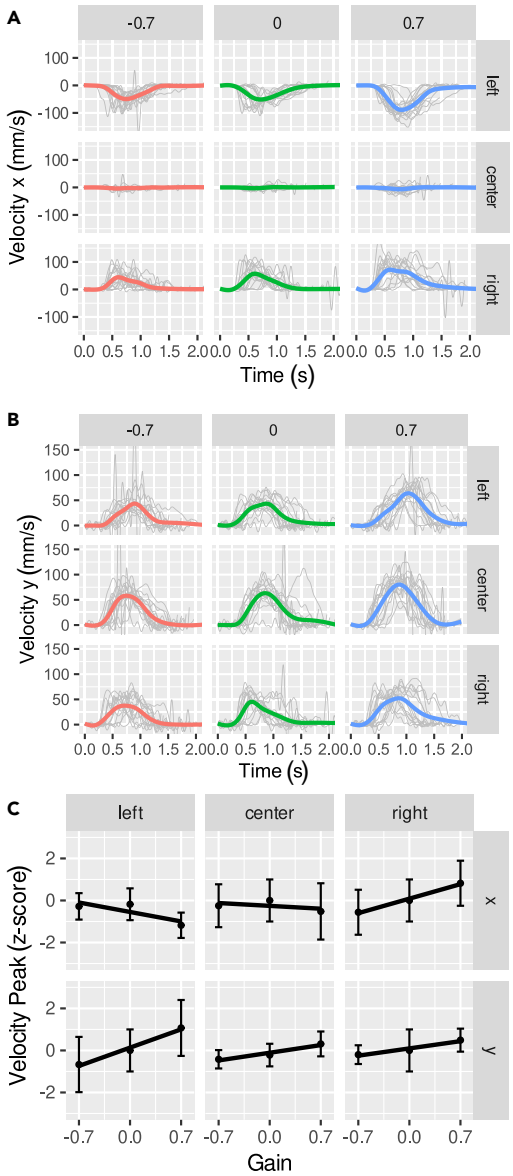

Figure 4. Velocity profile of a representative participant

The zero of the frame of reference corresponded to the starting position. Therefore, a leftward (rightward) movement of the finger correspond to a negative (positive) velocities along the x axis. Forward movements correspond to positive velocities along the y axis. (A) The different panels represent the velocity profile for the three target positions (labeled on the right border of the figure) and for the three values of gain (upper border). Data was pooled across trials and interpolated using GAM regression. In accordance with our model, we observed a lower peak velocity in negative gain conditions (red) and a higher peak velocity in positive gain conditions (blue), as compared to the baseline (green).

(B) Velocity profile along the y axis.

(C) The linear relation between peak velocity (*Z* score, mean ± SD) and gain is consistent with the one predicted by the observer model.

of interaction between lateral targets and x-gain were significant for the x axis (gain: left, Estimate = −0.48, $p < 0.001$, gain: right, Estimate = 0.54, $p < 0.001$). As expected, the x-gain did not affect movements toward the central target because in that case there were no lateral movements. The main effect of gain (i.e., central target - forward motion of the hand) was significant along the y axis (Estimate = 0.45, $p = 0.011$). Along the y axis the effect was slightly smaller for the left and right target due to the oblique movements of the hand, although the difference was not statistically significant.

As for the velocity peak, also the final position was significantly affected by the values of gain (Figures S5 and S6; Tables S7 and S8). The two terms of interaction between lateral targets and x-gain were significant for the x axis (gain: left, Estimate = −13.6, $p < 0.001$, gain: right, Estimate = 20.8, $p < 0.001$). The x-gain did not affect movements toward the central target because in that case there were no lateral

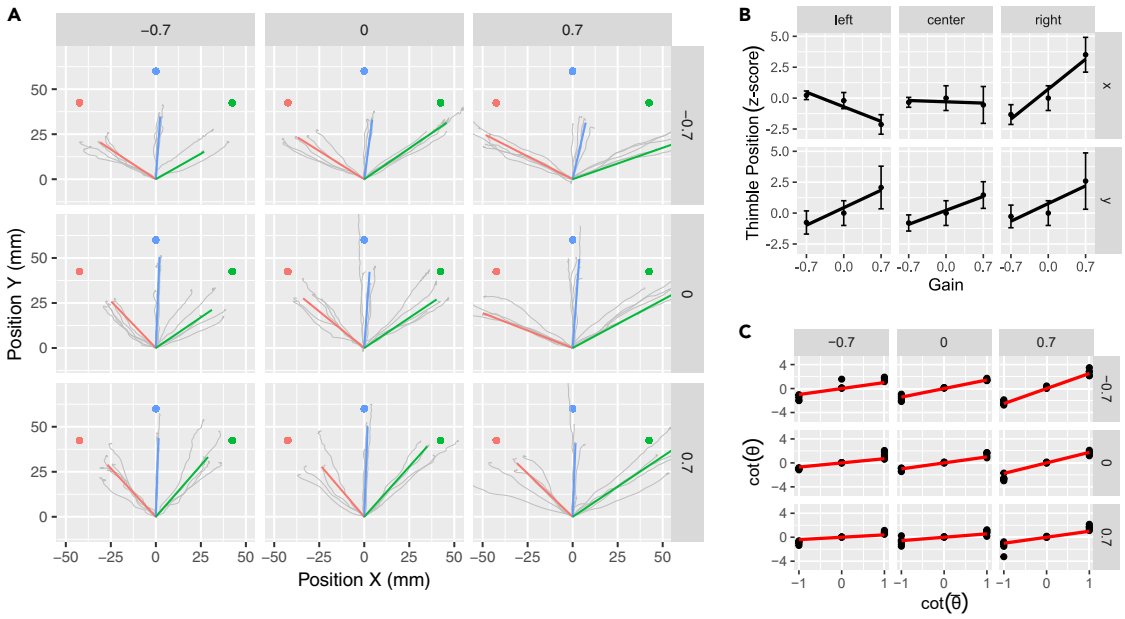

Figure 5. Results for a representative participant from experiment 1

(A) Motion paths for all combinations of x- and y-gain. The left, center and right target are shown in the colors red, blue, and green respectively. In accordance with model predictions, the gain affected both, the path length and the motion angle.

(B) Linear relationship between the final position of the finger (*Z* score, mean ± SD) and the gain value along the x- and the y axis.

(C) The relationship between the cotangent of the desired and the observed motion angle, for each combination of gain.

movements. Along the y axis, the main effect of gain (central target - forward motion of the hand) was statistically significant (Estimate = 14.7, $p < 0.001$). The effect was smaller for the left ($p = 0.07$) and right target ($p = 0.004$) due to the oblique movements of the hand. For completeness, we replicated the same analysis in the high force subset of data (peak forces equal or higher than threshold values) with comparable results (Figure S2; Tables S5, S6, S9, and S10). Refer to supplemental information for further details on the analysis of forces.

Experiment 2: Visual control experiment

In the first experiment, we observed systematic errors in reaching movements when the gain was not zero that were in accordance with the predictions of our model. We hypothesized that errors were due to an incorrect estimate of hand velocity following the change in tactile slip motion produced by the robotic device. Therefore, including an additional reliable cue should reduce the effect described in the first experiment. We ran a second experiment to investigate changes in motor errors when reliable visual feedback was given regarding hand trajectory. This experiment was similar to the main experiment with the exception that a dot on the PC monitor provided continuous visual feedback to the participants on the finger position and motion. This additional cue would reduce the value of the weight of the tactile channel. Hence, we expected a substantial reduction in the reaching errors if these depended on the altered tactile feedback.

Hand velocity

As in experiment 1, the velocity profiles were bell-shaped and symmetrical. Overall, we observed that gain had only a minor effect on hand velocity. The effect of gain along the x axis was not statistically significant for the right target with respect to the central target (Estimate = 0.07, *p*-value = 0.41), whereas a significant effect remained for the left target (Estimate = −0.38, *p*-value <0.001). For reaching movement toward the central target the gain did not produce any effect (Estimate = 0.082, *p*-value = 0.18). The effect of gain on the y axis was not statistically significant for any of the three targets (Estimate = 0.02, *p*-value = 0.70). The predicted slope of the LMM is illustrated for the whole sample and for each participant in Figures S11 and S12, for the x and the y axis, respectively.

Motion path and path length

Differently from experiment 1, the motion path length did not differ significantly depending on the gain condition (Figures 8A and 8B). The effect of gain was about 10 times smaller than in experiment 1. Specifically, along the x axis the slope of the linear regression was zero for the central target (Estimate = −0.05, *p*-value = 0.91), positive for the right target (Estimate diff. = 1.7, *p*-value = 0.008), negative for the left target (Estimate diff. = −0.83, *p*-value = 0.2). Along the y axis, the effect of the gain was not significantly different from zero (Estimate = −0.42, *p*-value = 0.51). There was no significant interaction between gain and right target (Estimate = 1.38, *p*-value = 0.14), and gain and left target

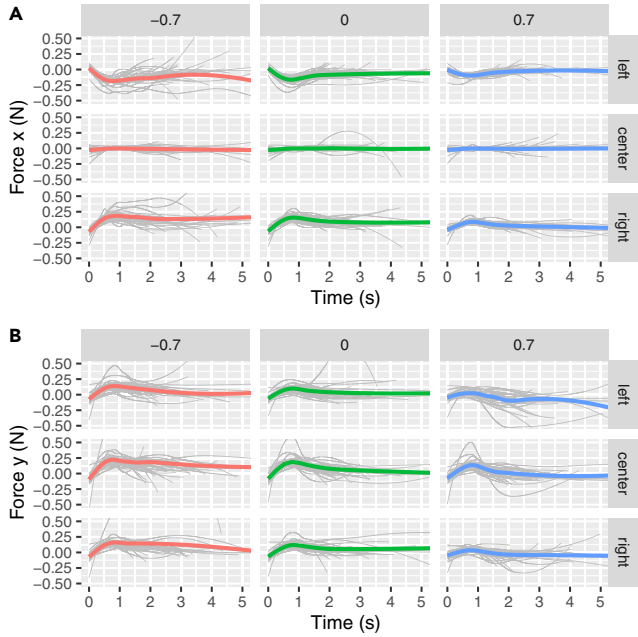

Figure 6. The average profile of shear force over time in the nine gain conditions in Experiment 1, for the x (A) and the y axis (B)

Gray lines represent average profiles for individual participants. Positive, zero and negative values of gain are represented in blue, green, and red, respectively. Average force over time for individual participants (gray lines) is obtained by fitting splines to the data. The population-level representations (shown by the colored lines) are obtained by calculating the spline fittings across individual participants.

(Estimate = 1.40, *p*-value = 0.13). The predicted slope of the LMM is illustrated for the whole sample and for each participant in Figures S13 and S14, for the x and the y axis, respectively.

Motion angle

We computed the cotangent of the motion angle and of the desired angle and fit the nonlinear model in Equation 1 to the data as in experiment 1. Figure 8C shows the motion angles in the same representative participant as in experiment 1. The fitted values of w_c across participants was equal to 0.08 ± 0.11 (Mean $\pm$ Standard Deviation). We ran a two-sample t-test and found that the weight of the tactile channel, w_c was significantly different between the two experiments (difference = 0.38, t = 6.76, *p*-value = <0.001).

Force

The distribution of forces was similar to the first experiment (compare Figures S15 and S16 for the two experiments). There was a significant association between the tactile slip velocity and tangential force, such that the faster the slip motion, the higher the module of the force (x axis, Estimate = 0.001, $p < 0.001$; y axis, Estimate = 0.0007, $p < 0.001$). The tangential force was also significantly associated with the load force (x axis: Estimate = 0.1, $p < 001$; y axis: Estimate = 0.21 $p < 001$).

Experiment 3 and rating experiment: Role of tactile acuity and shear force

In Experiment 3, we investigated the role of tactile sensitivity and shear forces on motor errors. This experiment consisted of a reaching task without visual feedback (similar to the first experiment). Participants contacted the finely textured, lubricated plate either with their bare fingertip, or with a rigid thimble covering their fingertip, which is known to reduce tactile sensitivity.[31–33] In two bare-fingertip conditions, the plate was lubricated either with ultrasound gel (resulting in a setting analogous to the one of the first experiment) or with seed oil, the latter having a higher friction coefficient than gel.[34,35] The ultrasound gel was also used as lubricant in the thimble condition. The experiment thus resulted in three conditions (labeled as *gel*, *oil*, and *thimble*), each one tested in a separate block. Each block included a subset of the conditions of gain factors and target positions used in Experiment 1 and 2 (see STAR Methods for details).

Tactile sensitivity

Rating experiment and motion angle. Prior to experiment 3, we conducted an independent rating experiment to obtain an explicit measure of tactile sensitivity in the conditions of *gel*, *oil*, and *thimble*. Participants were requested to explore the textured plate in each condition

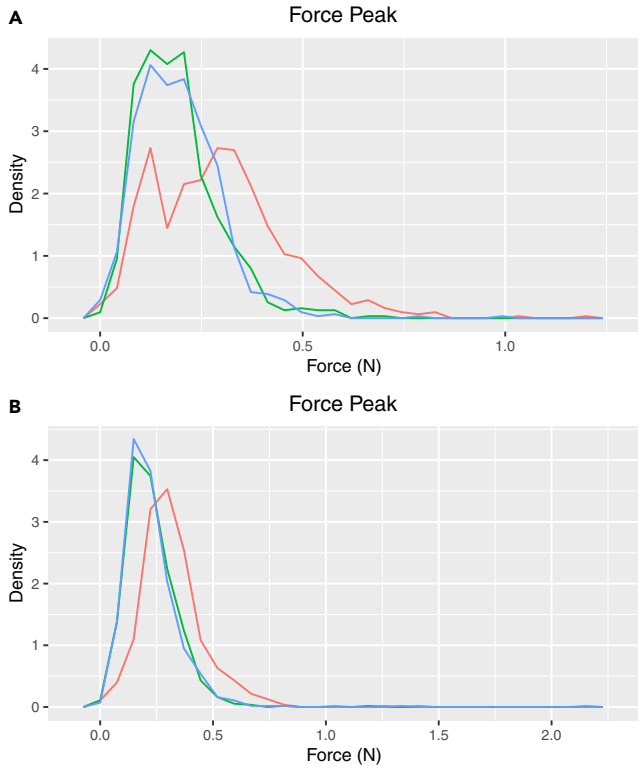

Figure 7. The distribution of the force peak in Experiment 1

The two panels represent the force peak for the x (A) and the y axis (B). Positive, zero, and negative values of gain are represented in blue, green, and red, respectively.

by sliding their fingertip on it. Afterward, they ranked the conditions from one ("it was difficult to distinguish the fine texture") to three ("it was easy to distinguish the fine texture"). They also scored each condition on a Likert scale from one (difficult) to seven (easy). Reported tactile sensitivity was highest in the *oil* condition followed by *gel* and then *thimble* (Figures 9A and 9B). The *thimble* condition was rated as the most difficult in both the ranking (1.2 ± 0.4; mean ± SD) and the scale rating (3.4 ± 1.5), followed by *gel* (ranking: 1.9 ± 0.6; scale: 4.7 ± 1.6) and *oil* (ranking: 2.9 ± 0.3; scale: 6.0 ± 0.8). We performed a Friedman test to evaluate whether the ranking and the scale ratings were significantly different between conditions. The effect of condition was statistically significant in both ratings (for ranks: Friedman chi-squared = 14.6, df = 2, p-value <0.001; for scales: Friedman chi-squared = 12.8, df = 2, p-value = 0.0017).

Next, participants (n = 17) performed the reaching task in the three conditions (*gel*, *oil*, and *thimble*) described above. To obtain an implicit measure of tactile sensitivity from this experiment, we estimated the tactile weight w_c from the analysis of the motion angle, using the methodology described in Experiment 1 (Figure 9E). We found that w_c was significantly greater in the *gel* condition compared to the *thimble* condition (paired t-test; difference = −0.23, t = 3.97, p = 0.001). Conversely, the difference between the *oil* and the *gel* condition was not statistically significant (difference = 0.04, t = −0.47, p = 0.64).

As anticipated, the *thimble* condition was the most challenging in terms of tactile discrimination, and such a result was supported by both implicit and explicit measures of tactile sensitivity. In the case of the *oil* condition, we have partial consistency between the two measures: while explicit assessments indicate significantly higher tactile sensitivity in the *oil* compared to the *gel* condition, the implicit measure does not yield a significant difference, although the order between the two conditions is maintained.

Force

To evaluate changes in shear forces between the different conditions, we measured the peak values of the forces along the x and y axis. By means of LMMs, we found that the values of shear forces were lower in the *gel* condition as compared to both the *oil* and *thimble* conditions (Figures 9C and 9D). Specifically, the peak force along the x axis was significantly higher in the *oil* condition (difference: 0.09 ± 0.006 N, p <0.001) and in the *thimble* condition (difference: 0.03 ± 0.006 N, p <0.001) as compared to the *gel* condition. Results were similar along the y axis: the peak force was significantly higher in the *oil* (difference: 0.12 ± 0.007 N, p <0.001) and in the *thimble* condition (difference: 0.13 ± 0.007 N, p <0.001) as compared to the *gel* condition. In accordance with the first experiment, the shear forces were significantly lower when the plate was following the hand (gain = 0.7) than when moving opposite to it (gain = −0.7) in all conditions. In the x axis the difference between gain values was −0.17 ± 0.0046 N (Estimate ± Std. Error, p <0.001), and the y axis difference was −0.06 ± 0.006 N

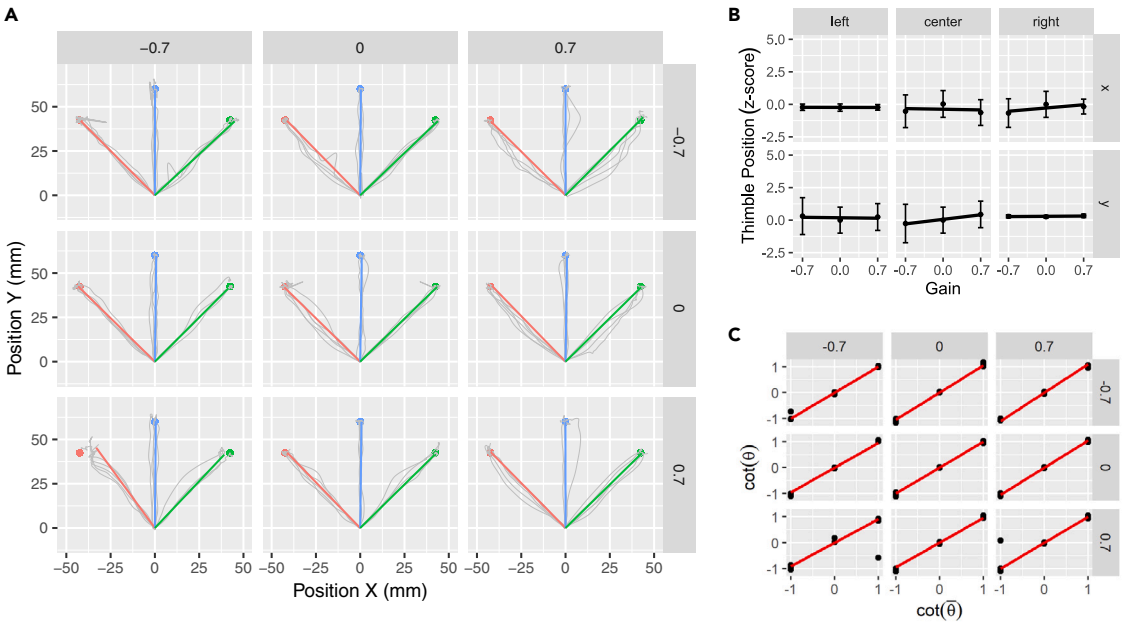

Figure 8. Results from a representative participant in Experiment 2

(A) Motion paths for all combinations of x and y gain. The left, center, and right target are shown in the colors red, blue and green respectively.

(B and C) Both the final position of the finger (Z score, mean ± SD in panel b) and the observed motion angle (panel c) were independent from the value of gain.

($p < 0.001$). The higher shear forces observed in the *oil* condition align with the expectation, given that the friction coefficient of seed oil is higher than that of ultrasound gel. However, we also observed an increase in shear forces in the *thimble* condition compared to the *gel* condition.

Hand velocity and positional error

As in the other experiments, we analyzed separately the results relative to hand velocity and motion trajectories. Specifically, we compared the effects associated with the change in the gain factor along the x and y axes, across the three experimental conditions: gel, oil, and thimble. Since we did not include the central target in Experiment 3 (see Method details in STAR Methods), the results for the left and the right target were analyzed together by considering the absolute values of peak velocity and final position.

We used LMMs to evaluate how the different values of gain affected the motion velocity and the motion path in the three experimental conditions of *gel*, *oil*, and *thimble*. In accordance with the first experiment, in the *gel* condition the effect of gain significantly affected both the final position ($p < 0.001$) and the peak velocity ($p < 0.001$), and the effects were similar for the x and the y axes. Notably, there were differences in the *oil* and *thimble* conditions with respect to the *gel* condition in terms of the effects of gain on both the peak velocity and the final positional error.

For the peak velocity (Figure 10A), the effect of gain along the x axis was significantly smaller in the *thimble* than in the *gel* condition (−0.17 ± 0.06; $p = 0.001$) and was non-significantly different between the *gel* and the *oil* condition (difference estimate <0.01, $p = 0.96$). Along the y axis the differences between conditions were not statistically significant ($p = 0.13$ for the difference between gains in thimble and gel conditions; $p = 0.82$ for the difference between gains in oil and gel conditions).

For the final positional error (Figure 10B), the effect of gain along the x axis was significantly smaller in the *thimble* than in the *gel* condition (−5.8 ± 0.87, Estimate ± Std. Error; $p < 0.001$), and it was slightly larger in the oil than in the gel condition, although this second comparison was not statistically significant (1.1 ± 0.89; $p = 0.23$). Along the y axis, the effect of gain on the final position was significantly smaller in the *thimble* than in the *gel* condition (−2.9 ± 0.81; $p < 0.001$), and it was significantly larger in the *oil* than in the *gel* condition (1.8 ± 0.83; $p = 0.03$). Figure 10C shows the motion paths of a representative participant across the two target positions (left and right), including the four possible combinations of x and y gain, and the three experimental conditions tested in experiment 3.

In summary, we found that the effect of gain on peak velocity was similar in the oil condition compared to the gel condition. Although numerically larger in the oil condition, the effect of gain did not yield significant differences between the two conditions. Regarding positional error, a similar trend in response to gain was observed in the oil and gel conditions, with significant differences along the y axis. Conversely, in the thimble condition compared to the gel condition, the influence of gain on peak velocity appeared smaller, particularly along the x axis where significant differences were observed. This trend also emerged in positional error, with gain having a significantly smaller effect in the thimble condition relative to the gel condition along both axes.

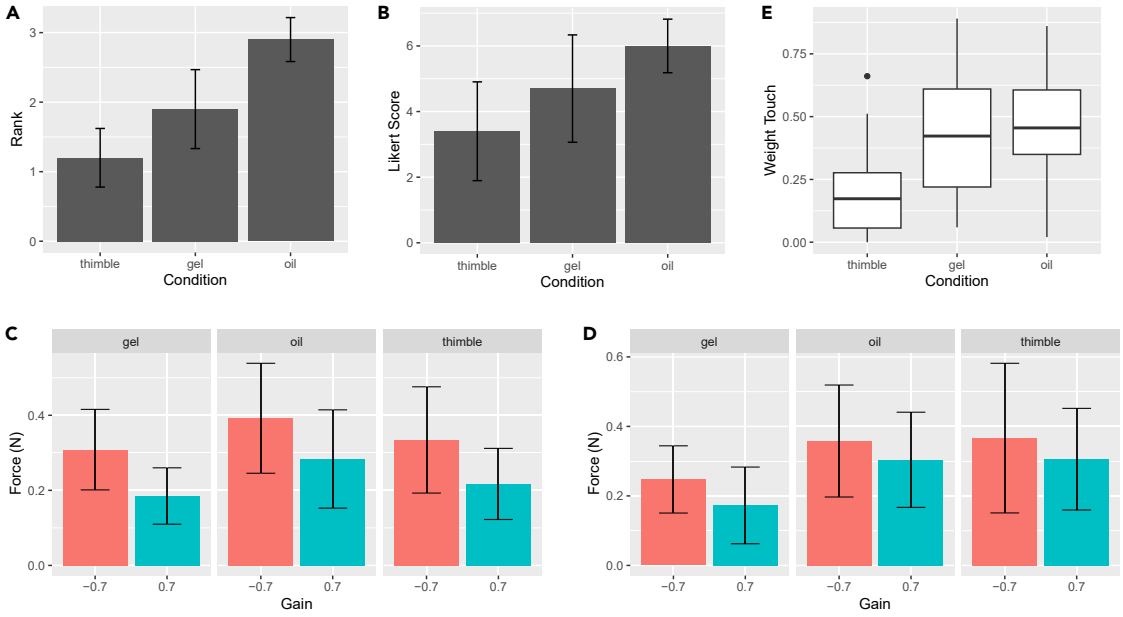

Figure 9. Results of the rating experiment and force peak in Experiment 3

(A and B) Rank and score by condition (mean values and standard deviations) according to participants. (C and D) Values of shear force (mean values and standard deviations) along the x axis and y axis. (E) Weight of touch (quantiles) by condition as estimated by the model.

DISCUSSION

Manipulation and exploration are two primary objectives that are commonly identified from the interaction with objects. Manipulation refers to the purposeful handling or adjustment of objects, often with the goal of achieving a specific task or function. Exploration, on the other hand, involves the act of interacting with objects to gain a deeper understanding of their properties, textures, or qualities. A less-acknowledged third aim in such interactions is to obtain information about the movement of our limbs during contact with objects, also referred to as extrasomatic information.[32,36] Contact with objects can be seen as an auxiliary proprioceptive cue, adding a dimension of self-awareness and sensory feedback to our interactions with the external world. Extrasomatic cues may possibly account for the reaching movements being generally planned with respect to the hand.[3,10,37,38] Accordingly, when reaching different targets in 2D, both the endpoint distribution of the hand around the target[3] and the velocity profile of the hand[39] have a stereotyped and characteristic shape. Electrophysiology studies showed that the direction of hand reaching is predicted by the population vector of the pool of motor neurons in the primary motor cortex (M1).[39,40] The response of individual neurons is related to the motion direction of the end-effector during both movement planning and execution.[41,42]

Because of this hand centered reference frame, we hypothesized that the spatial configuration and motion of the touched surface would be of primary importance in the control of reaching movements. In accordance with this hypothesis, we demonstrated that reaching movements can be systematically biased when the contact surface also moves, that is, when prior assumption that objects are stationary is violated. To this aim, we used a novel robotic device to control the position of a plate based on the displacement of the hand sliding on it. It was possible to decouple slip motion from proprioception by modifying the gain between plate and hand position. This altered tactile stimulus produced a bias in the reaching movement. As in previous studies,[38,43] participants demonstrated the typical bell-shaped velocity profile. However, in our task the peak velocity was affected by the gain parameter—in accordance with our hypothesis. Specifically, higher peak velocities were observed with positive gain conditions, when the plate was following hand movement, and lower peak velocities were observed with negative gain conditions, with the plate moving opposite to the hand. Motion paths and angles were also affected by the gain. A positive gain along the x or the y axis produced an overly long path along that axis as compared to a negative gain. Furthermore, our results demonstrated a nonlinear relationship between the desired angle, the actual motion angle, and the gain, consistent with the predictions of our model. The direction of movement—whether toward or away from the body mid-line—could explain the asymmetry observed in the findings of this study. Specifically, in the initial position, the hand and fingertip were aligned with the right shoulder. Leftward movements were directed from this starting position toward the body mid-line, while rightward movements were directed away from it. This is in accordance with prior research showing a dependency between arm posture with respect to the body's mid-line and the perception of arm and hand displacement, during both active and passive tasks.[44,45]

Previous studies evaluated reaching trajectories in presence of external force fields produced by a robotic interface.[11–15] In these studies, typically participants held a manipulandum and reached toward a target on a plane, while the manipulandum perturbed the participant's movements with a pattern of velocity-dependent forces, without tactile slip motion. Participants significantly deviated from the straight path when the external force field was first applied.[11,13] Even in the absence of visual feedback, corrective movements occurred to

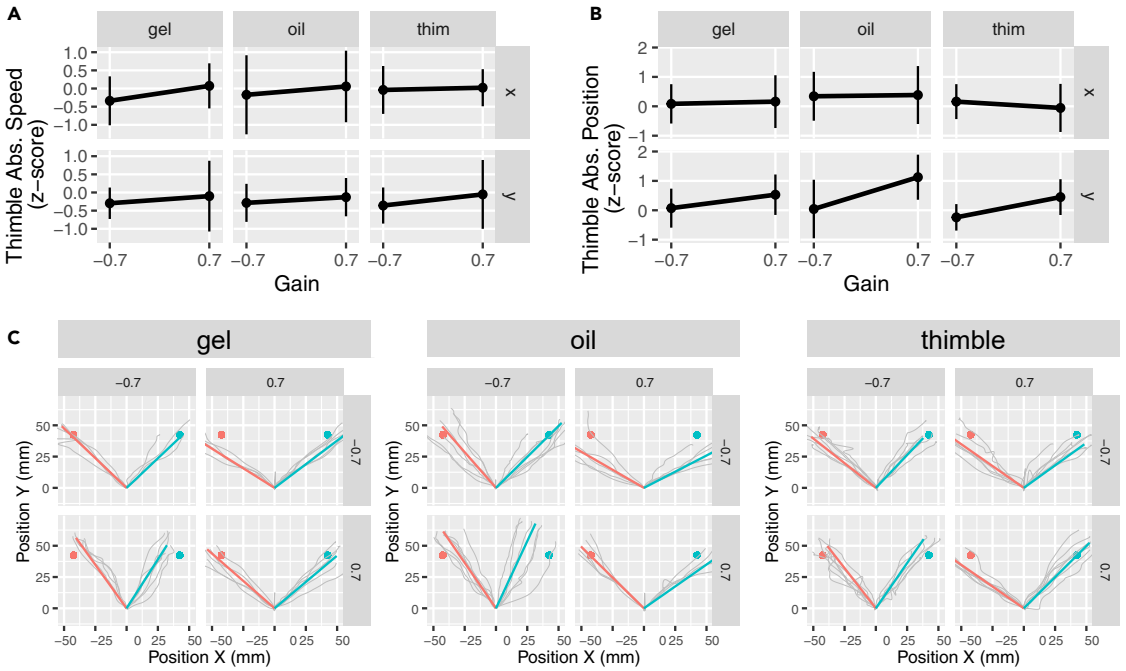

Figure 10. Results for a representative participant from experiment 3

(A) The linear relation between absolute value of peak velocity (*Z* score, mean ± SD) and gain for the three conditions in the experiment, along the x- and y axis.

(B) The same linear relation for the absolute value of final position (*Z* score, mean ± SD).

(C) Motion paths for all combinations of x- and y-gain in all the experimental conditions. The left and right targets are shown in the colors red and green, respectively.

compensate for the errors caused by the unexpected field leading to the characteristic curved path. These corrective movements are possibly based on proprioceptive information detecting the error or on viscoelastic properties of the muscles.[11] Noticeably, correction movements were not observed in our experiment 1 and 3 of the current study (i.e., without visual feedback), consistent with the hypothesis that participants moved along the desired trajectory estimated from the integration of proprioception and touch. In previous studies participants were able to efficiently compensate for the external perturbation when the same force field was presented across multiple trials.[12,13,15,46] Instead, perturbations were presented in random order in our study. In future work it may be interesting to evaluate the possible adaptation to the gain conditions used in the current study for repeated exposure to the same perturbation.

The results of our study are consistent with previous findings that tactile slip motion is a cue to the control of reaching movement.[10] In our previous study slip motion was biased by the orientation of a pattern of raised lines,[10] in accordance with the "aperture problem" predicted by the model of tactile flow.[22] According to this model, a vector field describes the flow of strain energy density in the human fingerpad. In the current study a surface with a fine homogeneous texture was used. In this case, the tactile flow model does not predict any bias in the perceived motion direction, since local contributions of the vector field are aligned with relative motion. Instead, the violation of the stationarity assumption produced the systematic error in reaching movement in the current task. In future work, it would be interesting to further investigate how the effect of aperture-related illusions due to heterogeneous patterns,[22,47] and those related to non-stationarity, are integrated.

In general, the values of shear forces were small in all conditions due to the use of Teflon and the presence of the lubricant on the contact plate. Therefore, it is unlikely that the motor errors were due to the mechanical perturbation caused by the moving plate. The results of the study were confirmed when restricting the analysis to a subset of data where shear forces were small and homogeneous across gain conditions (less than 0.25 N and less than 0.21 N for the x and the y axis, respectively). Notably, we found similar effects within this subset compared to those observed across the entire dataset. Had the impact of gain on motor response been proportional to shear forces, we would have expected distinct patterns of the effects of gain on motor errors within the considered subset. Nevertheless, a minor role of shear forces in modulating the effects driven by tactile sensitivity cannot be excluded, and it represents a promising direction for future investigation. The effects of the moving plate were negligible when accurate visual feedback was provided to the participants (experiment 2). Finally, a third experiment was conducted with the aim of examining how varying shear force conditions and tactile acuity levels affect hand trajectory. Our findings revealed notable differences across the different conditions of this third experiment. We observed that the shear forces were significantly lower in the gel condition when compared to both the thimble and oil conditions. Instead, tactile acuity presented a different pattern. While explicit metrics revealed that tactile acuity was highest in the *oil* condition, implicit measurements showed comparable acuity to the *gel* condition. Conversely, the *thimble* condition consistently exhibited the lowest tactile acuity across both explicit and implicit measures. Tactile acuity self-reported with the Likert scale may be different from implicit processing of tactile

stimuli for motor control. However, combining implicit evaluation and questionnaires is a common method in psychophysical investigations and user studies.[48]

Notably, the effect of gain on motor errors was proportional to tactile acuity, with the most substantial effect of gain in the oil condition and the least pronounced effect in the thimble condition. This outcome can be attributed to the inherent bias introduced by the tactile information provided through touch, which is influenced by the violation of a static prior. As a result, this bias has a diminished impact in conditions where the tactile information is less reliable (thimble condition), as predicted by Equation 1. Overall, our study provides support for the hypothesis that the bias in hand trajectory is a consequence of the modified tactile information stemming from the artificial movement of the surface of the device. Given the inherent complexity of mechanical stimuli, it remains challenging to isolate specific elements. It is possible that additional factors, such as local skin deformation including partial slips and deformation rate, may also play a role in influencing the observed effects. Further investigation is necessary to elucidate these potential contributions.

The perceptual system integrates sensory measurements with prior knowledge about the world, so as to increase the precision of the combined estimate.[25,49] As mentioned before, in daily interaction with inanimate objects observers assume *a priori* that these are stationary or in slow motion, and a Bayesian model was developed to take this assumption into account.[24,25] This model was able to predict several perceptual illusions in vision[24,25] and was later extended to other sensory domains including the somatosensory,[27] the auditory,[50] and the vestibular system.[51] Fitting the slow-motion prior model to psychophysical data accurately predicts the neural tuning characteristics for visual speed in brain area MT.[52] In our model the slow-motion prior was not explicitly included; however, the integration process between touch and proprioception implies the assumption by the observer that the plate was not moving. Without this stationarity assumption, participants would have discarded the tactile cue, and no bias would be observed. Provided that the surface is stationary, tactile slip motion and kinesthetic cues are congruent and can be optimally integrated.

We modeled the integrated estimate of the hand velocity as a weighted sum of proprioception and touch. The weight of each sensory channel was estimated by the data, with the constraint that the sum of the weights is equal to one. This model can be extended to an optimal integration model provided that the noise associated with each sensory channel is specified.[53] Previous studies showed that observers optimally integrate vision and proprioception for the control of hand movement in reaching tasks.[7,8,14] The integrated estimate of the position of the hand lies on a curve joining the two bimodal Gaussian distributions. The whole hand trajectory during reaching could be predicted by a Kalman filter observer including a forward model of the motor command.[10,54] Results of our experiment 3 (thimble vs. gel condition) supported the hypothesis of optimal integration. In future work, optimal integration can be further evaluated with our task in people with tactile deficits, such as diabetic neuropathy[55] or Friedreich Ataxia. In the presence of a tactile deficit, participants may assign less weight to the tactile channel and be less sensitive to the effect of gain.

A violation of the stationarity assumption will become ever more frequent due to the emergence of novel forms of human-machine interactions enabled by the deployment of extended reality interfaces and collaborative robots (cobots). Therefore, studying reaching movements when the static prior is violated is important for understanding the sensorimotor control of the hand in a dynamic world. In addition, these studies could open interesting perspectives in extended reality applications, and more specifically in mixed reality environments. The goal of retargeting technologies is to devise haptic-based control strategies, to give to the user the illusory perception of reaching a virtual object, positioned in a certain place of the virtual scene, while she/he is reaching a real object positioned in another place with respect to the virtual one. This topic was pioneered in our previous work[56] and can be further developed leveraging on the findings of the current study.

Limitations of the study

The specifics of the haptic device[29,57] limited the velocity and the range of motion of the reaching task. To reduce the inertia of the device it would be possible to develop a wearable version of the device, which could significantly enhance its usability and applicability. Another possibility is to modify the existing control law of the robotic device used in the current work, by developing a force-based control for updating plate position, eventually relying on a nested control loop. This will help to further reduce the tracking error between the desired and the current position of the plate and to monitor the force exerted by the finger on the plate.

A major challenge of the study was to disentangle the mechanical perturbation to the arm produced by tangential forces (friction) and the sensory effects arising from the altered slip motion. We used different strategies to mitigate this potential confound: in the first experiment, we restricted the analysis to a subset of data with low tangential forces; in the third experiment, we compared different types of lubricants, and we reduced tactile sensitivity by covering the fingertip with a thimble. The following limitations of the third experiment need to be considered. In the thimble condition, limited tactile information was still available to the participants (similarly to what would occur when exploring the surface of an object using a rigid tool or a thick glove). Residual frictional forces remained despite applying different lubricants, detailed in the results section of the manuscript. Given the inherent complexity of tactile motion, present at every stage from contact mechanics to perceptual processing, it remains challenging to isolate the contribution of its specific elements to the observed phenomenon. Specifically, slip motion in absence of friction is only possible in special cases, for example using pin-based tactile displays. The interpretation of the results of the study as due to "pure" tactile motion (i.e., tactile motion in the absence of friction) cannot be ensured with the specific experimental approach that is based on the real motion of the contact surface. Despite these limitations, we believe that the low values of frictional forces may have contributed to a limited extent to the main effects that we reported, which mainly depended on the violation of the stationarity assumption.

Finally, the long-term implications of our findings on human-robot collaboration and the adaptability of human sensorimotor systems remain speculative. More research is needed to explore the practical applications and potential challenges that may arise in environments where objects deviate from assumed principles of stationarity.

STAR★METHODS

Detailed methods are provided in the online version of this paper and include the following:

- KEY RESOURCES TABLE
- RESOURCE AVAILABILITY
  - Lead contact
  - Materials availability
  - Data and code availability
- EXPERIMENTAL MODEL AND STUDY PARTICIPANT DETAILS
- METHOD DETAILS
  - Experimental setup
  - Control algorithm
- QUANTIFICATION AND STATISTICAL ANALYSIS
  - Predictions of the vector model

SUPPLEMENTAL INFORMATION

Supplemental information can be found online at https://doi.org/10.1016/j.isci.2024.109871.

ACKNOWLEDGMENTS

We would like to thank Cesare V. Parise for useful comments and suggestions on the manuscript and Giulia Daniele, Fanny Valente, and Alice Flamini for data collection.

This study was partially supported by the Italian Ministry of Health (Ricerca corrente, IRCCS Fondazione Santa Lucia, Ricerca Finalizzata RF-2018-12365985), the Italian Space Agency (grant I/006/06/0), INAIL (BRIC 2022 LABORIUS), the Italian Ministry of University and Research (MIUR) (PRIN grant 20208RB4N9_002, 2020EM9A8X_003, and 202249C5XL and in the framework of the FoReLab project - Departments of Excellence), the European Commission H2020 Framework Programme (HARIA, grant no. 101070292 and EXPERIENCE, grant no. 101017727); the European Research Council ERC (Natural BionicS, grant no. 810346), and by the Next Generation EU Project (NGEU) ECS00000017 'Ecosistema dell'Innovazione' Tuscany Health Ecosystem (THE, PNRR, Spoke 9: Robotics and Automation for Health) and Next Generation EU Project (NGEU) National Recovery and Resilience Plan (NRRP), project MNESYS (PE0000006) – A Multiscale integrated approach to the study of the nervous system in health and disease (DN. 1553 11.10.2022) Spoke 1.

AUTHOR CONTRIBUTIONS

Conceptualization, C.P.R., S.C., A.B., F.L., M.B., and A.M.; Methodology, C.P.R., S.C., P.B., M.B., and A.M.; Software, S.C.; Investigation, C.P.R. and S.C.; Visualization, C.P.R., P.B., and A.M.; Writing – Original Draft, C.P.R. and A.M.; Writing – Review and Editing, C.P.R., S.C., P.B., F.L., M.B., and A.M.; Funding Acquisition, A.B., F.L., M.B., and A.M.; Resources, A.B., F.L., M.B., and A.M.; Supervision, A.B., F.L., M.B., and A.M.

DECLARATION OF INTERESTS

The authors declare no competing interests.

Received: February 14, 2023
Revised: November 10, 2023
Accepted: April 29, 2024
Published: May 2, 2024

REFERENCES

1. Lederman, S.J., Klatzky, R.L., and Barber, P.O. (1985). Spatial and movement-based heuristics for encoding pattern information through touch. J. Exp. Psychol. Gen. *114*, 33–49. https://doi.org/10.1037/0096-3445.114.1.33.
2. Lederman, S.J., and Klatzky, R.L. (1987). Hand movements: A window into haptic object recognition. Cogn. Psychol. *19*, 342–368. https://doi.org/10.1016/0010-0285(87)90008-9.
3. Gordon, J., Ghilardi, M.F., Ghez, C., and Ghez, C. (1994). Accuracy of planar reaching movements I. Independence of direction and extent variability. Exp. Brain Res. *99*, 97–111. https://doi.org/10.1007/BF00241415.
4. Izawa, J., Rane, T., Donchin, O., and Shadmehr, R. (2008). Motor adaptation as a process of reoptimization. J. Neurosci. *28*, 2883–2891. https://doi.org/10.1523/JNEUROSCI.5359-07.2008.
5. Sober, S.J., and Sabes, P.N. (2003). Multisensory integration during motor planning. J. Neurosci. *23*, 6982–6992. https://doi.org/10.1523/JNEUROSCI.23-18-06982.2003.
6. Sainburg, R.L., Ghez, C., and Kalakanis, D. (1999). Intersegmental dynamics are controlled by sequential anticipatory, error correction, and postural mechanisms. J. Neurophysiol. *81*, 1045–1056. https://doi.org/10.1152/jn.1999.81.3.1045.
7. Van Beers, R.J., Sittig, A.C., and Gon, J.J. (1999). Integration of proprioceptive and visual position-information: An experimentally supported model. J. Neurophysiol. *81*, 1355–1364. https://doi.org/10.1152/jn.1999.81.3.1355.
8. Körding, K.P., and Wolpert, D.M. (2004). Bayesian integration in sensorimotor learning. Nature *427*, 244–247. https://doi.org/10.1038/nature02169.
9. Pruszynski, J.A., Johansson, R.S., and Flanagan, J.R. (2016). A Rapid Tactile-Motor

Reflex Automatically Guides Reaching toward Handheld Objects. Curr. Biol. *26*, 788–792. https://doi.org/10.1016/j.cub.2016.01.027.
10. Moscatelli, A., Bianchi, M., Ciotti, S., Bettelani, G.C., Parise, C.V., Lacquaniti, F., and Bicchi, A. (2019). Touch as an auxiliary proprioceptive cue for movement control. Sci. Adv. *5*, eaaw3121. https://doi.org/10.1126/sciadv.aaw3121.
11. Shadmehr, R., and Mussa-Ivaldi, F.A. (1994). Adaptive representation of dynamics during learning of a motor task. J. Neurosci. *14*, 3208–3224. https://doi.org/10.1523/JNEUROSCI.14-05-03208.1994.
12. Li, C.S., Padoa-Schioppa, C., and Bizzi, E. (2001). Neuronal correlates of motor performance and motor learning in the primary motor cortex of monkeys adapting to an external force field. Neuron *30*, 593–607. https://doi.org/10.1016/s0896-6273(01)00301-4.
13. Brashers-Krug, T., Shadmehr, R., and Bizzi, E. (1996). Consolidation in human motor memory. Nature *382*, 252–255. https://doi.org/10.1038/382252a0.
14. Ikegami, T., Flanagan, J.R., and Wolpert, D.M. (2022). Reach adaption to a visuomotor gain with terminal error feedback involves reinforcement learning. PLoS One *17*, e0269297. https://doi.org/10.1371/journal.pone.0269297.
15. Nozaki, D., Kurtzer, I., and Scott, S.H. (2006). Limited transfer of learning between unimanual and bimanual skills within the same limb. Nat. Neurosci. *9*, 1364–1366. https://doi.org/10.1038/NN1785.
16. Pruszynski, J.A., Flanagan, J.R., and Johansson, R.S. (2018). Fast and accurate edge orientation processing during object manipulation. Elife *7*, e31200. https://doi.org/10.7554/eLife.31200.
17. Moscatelli, A., Naceri, A., and Ernst, M.O. (2014). Path integration in tactile perception of shapes. Behav. Brain Res. *274*, 355–364. https://doi.org/10.1016/j.bbr.2014.08.025.
18. Klatzky, R.L. (1999). Path completion after haptic exploration without vision: implications for haptic spatial representations. Percept. Psychophys. *61*, 220–235. https://doi.org/10.3758/BF03206884.
19. Fardo, F., Beck, B., Cheng, T., and Haggard, P. (2018). A mechanism for spatial perception on human skin. Cognition *178*, 236–243. https://doi.org/10.1016/j.cognition.2018.05.024.
20. Farajian, M., Leib, R., Kossowsky, H., Zaidenberg, T., Mussa-Ivaldi, F.A., Nisky, I., and Vaadia, E. (2020). Stretching the skin immediately enhances perceived stiffness and gradually enhances the predictive control of grip force. Elife *9*, e52653. https://doi.org/10.7554/ELIFE.52653.
21. Cataldo, A., Dupin, L., Dempsey-Jones, H., Gomi, H., and Haggard, P. (2022). Interplay of tactile and motor information in constructing spatial self-perception. Curr. Biol. *32*, 1301–1309.e3. https://doi.org/10.1016/j.cub.2022.01.047.
22. Bicchi, A., Scilingo, E.P., Ricciardi, E., and Pietrini, P. (2008). Tactile flow explains haptic counterparts of common visual illusions. Brain Res. Bull. *75*, 737–741. https://doi.org/10.1016/j.brainresbull.2008.01.011.
23. Bettelani, G.C., Moscatelli, A., and Bianchi, M. (2019). Contact with sliding over a rotating ridged surface: The turntable illusion. In 2019 IEEE World Haptics Conference (WHC), Tokyo, Japan, pp. 562–567. https://doi.org/10.1109/WHC.2019.8816119.
24. Weiss, Y., Simoncelli, E.P., and Adelson, E.H. (2002). Motion illusions as optimal percepts. Nat. Neurosci. *5*, 598–604. https://doi.org/10.1038/nn858.
25. Stocker, A.A., and Simoncelli, E.P. (2006). Noise characteristics and prior expectations in human visual speed perception. Nat. Neurosci. *9*, 578–585. https://doi.org/10.1038/nn1669.
26. Freeman, T.C.A., Champion, R.A., and Warren, P.A. (2010). A bayesian model of perceived head-centered velocity during smooth pursuit eye movement. Curr. Biol. *20*, 757–762. https://doi.org/10.1016/j.cub.2010.02.059.
27. Moscatelli, A., Hayward, V., Wexler, M., and Ernst, M.O. (2015). Illusory Tactile Motion Perception: An Analog of the Visual Filehne Illusion. Sci. Rep. *5*, 14584. https://doi.org/10.1038/srep14584.
28. Moscatelli, A., Scotto, C.R., and Ernst, M.O. (2019). Illusory changes in the perceived speed of motion derived from proprioception and touch. J. Neurophysiol. *122*, 1555–1565. https://doi.org/10.1152/jn.00719.2018.
29. Ciotti, S., Ryan, C.P., Bianchi, M., Lacquaniti, F., and Moscatelli, A. (2021). A novel device decoupling tactile slip and hand motion in reaching tasks: The HaptiTrack device. IEEE Trans. Haptics *14*, 248–253. https://doi.org/10.1109/TOH.2021.3075024.
30. Agresti, A. (2002). Categorical Data Analysis (John Wiley & Sons, Inc.). https://doi.org/10.1002/0471249688.
31. Kinoshita, H. (1999). Effect of gloves on prehensile forces during lifting and holding tasks. Ergonomics *42*, 1372–1385. https://doi.org/10.1080/001401399185018.
32. Moscatelli, A., Bianchi, M., Serio, A., Terekhov, A., Hayward, V., Ernst, M.O., and Bicchi, A. (2016). The change in fingertip contact area as a novel proprioceptive cue. Curr. Biol. *26*, 1159–1163. https://doi.org/10.1016/j.cub.2016.02.052.
33. Naceri, A., Gultekin, Y.B., Moscatelli, A., and Ernst, M.O. (2021). Role of tactile noise in the control of digit normal force. Front. Psychol. *12*, 612558. https://doi.org/10.3389/fpsyg.2021.612558.
34. Adhvaryu, A., Biresaw, G., Sharma, B.K., and Erhan, S.Z. (2006). Friction behavior of some seed oils: Biobased lubricant applications. Ind. Eng. Chem. Res. *45*, 3735–3740. https://doi.org/10.1021/ie051259z.
35. Haribabu, A., Surakasi, R., Thimothy, P., Khan, M.A., Khan, N.A., and Zahmatkesh, S. (2023). Study comparing the tribological behavior of propylene glycol and water dispersed with graphene nanopowder. Sci. Rep. *13*, 2382. https://doi.org/10.1038/s41598-023-29349-7.
36. Terekhov, A.V., and Hayward, V. (2015). The brain uses extrasomatic information to estimate limb displacement. Proc. Biol. Sci. *282*, 20151661. https://doi.org/10.1098/rspb.2015.1661.
37. Lacquaniti, F., and Soechting, J.F. (1982). Coordination of arm and wrist motion during a reaching task. J. Neurosci. *2*, 399–408. https://doi.org/10.1523/JNEUROSCI.02-04-00399.
38. Morasso, P. (1981). Spatial control of arm movements. Exp. Brain Res. *42*, 223–227. https://doi.org/10.1007/BF00236911.
39. Georgopoulos, A.P., Schwartz, A.B., and Kettner, R.E. (1986). Neuronal population coding of movement direction. Science *233*, 1416–1419. https://doi.org/10.1126/science.3749885.
40. Georgopoulos, A.P. (1995). Current issues in directional motor control. Trends Neurosci. *18*, 506–510. https://doi.org/10.1016/0166-2236(95)92775-L.
41. Pruszynski, J.A., Kurtzer, I., Nashed, J.Y., Omrani, M., Brouwer, B., and Scott, S.H. (2011). Primary motor cortex underlies multi-joint integration for fast feedback control. Nature *478*, 387–390. https://doi.org/10.1038/nature10436.
42. Churchland, M.M., Cunningham, J.P., Kaufman, M.T., Foster, J.D., Nuyujukian, P., Ryu, S.I., and Shenoy, K.V. (2012). Neural population dynamics during reaching. Nature *487*, 51–56. https://doi.org/10.1038/nature11129.
43. Goettker, A., Fiehler, K., and Voudouris, D. (2020). Somatosensory target information is used for reaching but not for saccadic eye movements. J. Neurophysiol. *124*, 1092–1102. https://doi.org/10.1152/jn.00258.2020.
44. Fuentes, C.T., and Bastian, A.J. (2010). Where is your arm? Variations in proprioception across space and tasks. J. Neurophysiol. *103*, 164–171. https://doi.org/10.1152/jn.00494.2009.
45. Kappers, A.M., and Koenderink, J.J. (1999). Haptic perception of spatial relations. Perception *28*, 781–795. https://doi.org/10.1068/p2930.
46. Gandolfo, F., Li, C., Benda, B.J., Schioppa, C.P., and Bizzi, E. (2000). Cortical correlates of learning in monkeys adapting to a new dynamical environment. Proc. Natl. Acad. Sci. USA *97*, 2259–2263. https://doi.org/10.1073/pnas.040567097.
47. Pei, Y.-C., Hsiao, S.S., and Bensmaia, S.J. (2008). The tactile integration of local motion cues is analogous to its visual counterpart. Proc. Natl. Acad. Sci. USA *105*, 8130–8135. https://doi.org/10.1073/pnas.0800028105.
48. Barontini, F., Obermeier, A., Catalano, M.G., Fani, S., Grioli, G., Bianchi, M., Bicchi, A., and Jakubowitz, E. (2023). Tactile feedback in upper limb prosthetics: A pilot study on trans-radial amputees comparing different haptic modalities. IEEE Trans. Haptics *16*, 760–769. https://doi.org/10.1109/TOH.2023.3322559.
49. Ernst, M.O., and Bülthoff, H.H. (2004). Merging the senses into a robust percept. Trends Cogn. Sci. *8*, 162–169. https://doi.org/10.1016/j.tics.2004.02.002.
50. Senna, I., Parise, C.V., and Ernst, M.O. (2015). Hearing in slow-motion: Humans underestimate the speed of moving sounds. Sci. Rep. *5*, 14054. https://doi.org/10.1038/srep14054.
51. Freeman, T.C.A., Culling, J.F., Akeroyd, M.A., and Brimijoin, W.O. (2017). Auditory compensation for head rotation is incomplete. J. Exp. Psychol. Hum. Percept. Perform. *43*, 371–380. https://doi.org/10.1037/xhp0000321.
52. Zhang, L.-Q., and Stocker, A.A. (2022). Prior expectations in visual speed perception predict encoding characteristics of neurons in area MT. J. Neurosci. *42*, 2951–2962. https://doi.org/10.1523/JNEUROSCI.1920-21.2022.
53. Körding, K.P., and Wolpert, D.M. (2006). Bayesian decision theory in sensorimotor control. Trends Cogn. Sci. *10*, 319–326. https://doi.org/10.1016/J.TICS.2006.05.003.
54. Wolpert, D.M., Ghahramani, Z., and Jordan, M.I. (1995). An internal model for

sensorimotor integration. Science *269*, 1880–1882. https://doi.org/10.1126/science.7569931.

55. Picconi, F., Ryan, C.P., Russo, B., Ciotti, S., Pepe, A., Menduni, M., Lacquaniti, F., Frontoni, S., and Moscatelli, A. (2022). The evaluation of tactile dysfunction in the hand in type 1 diabetes: A novel method based on haptics. Acta Diabetol. *59*, 1073–1082. https://doi.org/10.1007/s00592-022-01903-1.

56. Bettelani, G.C., Fani, S., Moscatelli, A., Salaris, P., and Bianchi, M. (2021). Controlling hand movements relying on tactile illusions: A model predictive control framework. In 2021 IEEE world haptics conference (WHC), pp. 985–990. https://doi.org/10.1109/WHC49131.2021.9517188.

57. Ciotti, S., Bianchi, M., Doria, D., Lacquaniti, F., and Moscatelli, A. (2022). HaptiTrack: A novel device for the evaluation of tactile sensitivity in active and in passive tasks. In Converging clinical and engineering research on neurorehabilitation IV, D. Torricelli, M. Akay, and J.L. Pons, eds. (Springer International Publishing), pp. 617–621. https://doi.org/10.1007/978-3-030-70316-5_99.

58. Bishu, R.R. (1993). Investigation of the Effects of Extravehicular Activity (EVA) Gloves on Performance (National Aeronautics; Space Administration, Office of Management).

STAR★METHODS

KEY RESOURCES TABLE

REAGENT or RESOURCE	SOURCE	IDENTIFIER
Deposited data		
Raw and analyzed data	This paper	https://doi.org/10.5281/zenodo.10964672
Code for analyzing data and generating figures	This paper	https://doi.org/10.5281/zenodo.11046295
Software and algorithms		
R version 4.3.1	The Comprehensive R Archive Network	cran.r-project.org
Python version 3.9.2	The Python Software Foundation	python.org
Unreal Engine 5	Unreal Engine	unrealengine.com
Motive Optical motion capture software	OptiTrack	optitrack.com/software/motive/
C++	The Standard C++ Foundation	isocpp.org/

RESOURCE AVAILABILITY

Lead contact

Further information and requests for resources should be directed to and will be fulfilled by the Lead Contact, Alessandro Moscatelli (a.moscatelli@hsantalucia.it).

Materials availability

This study did not generate new unique reagents.

Data and code availability

- All behavioral data of Experiment 1-3 have been deposited at Zenodo and are publicly available as of the date of publication. The DOI is listed in the key resources table.
- All original code (R code for analyzing data and generating figures) has been deposited at Zenodo and is publicly available as of the date of publication. The DOI is listed in the key resources table.
- Any additional information required to reanalyze the data reported in this paper is available from the lead contact upon request.

EXPERIMENTAL MODEL AND STUDY PARTICIPANT DETAILS

Human participants, predominantly comprising students attending the department's laboratories, took part in the experiments. No data regarding gender, ancestry, race, ethnicity, and socioeconomic status was collected. Participants did not report pathological conditions that would interfere with the measurements. The testing procedures for the experiment were approved by the ethics committee of the Santa Lucia Foundation (Prot. CE/PROG.898), in accordance with the guidelines of the Declaration of Helsinki for research involving human subjects. Informed written consent was obtained from all participants involved in the study. The sample size was set in accordance with previous studies in haptic literature.[9,10,14]

We tested 17 participants (8 female and 9 male participants; 14 naive participants and authors CPR, SC and AM) in the first experiment. Sixteen participants were right-handed. The age was equal to 28±6 yrs (mean ± standard deviation). In the second experiment we tested 16 participants (10 female and 6 male participants; 13 naive participants and authors CPR, SC and AM). The age was equal to 26± 5 yrs. Fifteen participants were right-handed. In the third experiment we tested 17 participants (13 female and 4 male participants; 15 naive participants and authors CPR and AM; 27±6 yrs). Ten naive participants were tested for the rating experiment (6 female and 4 male participants; 28± 5 yrs).

In three experiments, participants were requested to contact the movable plate of the apparatus and slide their fingertip to a target position displayed on a PC monitor in front of them (Figure 1A). Across trials, the position of the target was either to the left, to the center, or to the right with respect to the starting position (Figure 5). In the experiments, we tested three tactile slip motion conditions that were presented pseudo-randomly across trials. We used the R function sample() for randomizing the trials. In each of these conditions the position of the plate was updated according to the position of the hand multiplied by a gain factor (γ). This gain factor changed between these three conditions such that the plate was either stationary (i.e., control condition), following or moving opposite to hand motion. The details of the control algorithm used to set one the three conditions are described below.

METHOD DETAILS

Experimental setup

A multi-functional haptic device called HaptiTrack (Figure 1A) was developed to physically decouple tactile slip motion and hand movements. In this paragraph we describe the device in brief. The reader can refer to our previous publications for a more detailed description.[29,57] The device generates precisely controlled 2D motion of a contact plate, measures contact forces, and provides hand and finger tracking through an external tracking system. By means of a specific control algorithm described below, the velocity of tactile slip can be changed independently from the velocity of the hand sliding on the device's surface (maximum speed of 150 mm/s). The HaptiTrack device includes of a motion capture system (OptiTrack motion capture system with four Flex13 cameras and an OptiHub synchronization box), a sensorized plate, and two perpendicular linear motion axes actuated by DC-motors controlling the position of the plate. The motion capture system has a frame rate of 120 FPS, and a declared mean position reconstruction error less than 1 mm. The sensorized plate is mounted on the top of the apparatus (Figure 1B). The movement of the sensorized plate is produced by two perpendicular linear motion axes mounted on top of each other, similar to a 2D pantograph. To attenuate vibrations, four MISUMI damping components (GELB1401) are mounted between the top single-axis and the sensorized surface. For safety of the user, four proximity sensors (Panasonic GX-F12A) were attached to the extremities of the motion axes. This system will immediately interrupt the motors power supply if any of the proximity sensors is covered by any of the moving parts of the plate. Visual feedback is displayed on a PC monitor attached to the back side of the frame. A wood panel with a hole in the center (not shown in the figure) is mounted in the front side of the frame. A black curtain in front of the hole occludes the hand and the surface motion from sight. For each main hardware component a C++ library was developed under the 3-clause BSD license, a permissive free software license. A core C++ software with a sampling rate of 200 Hz integrates the signals from all the different modules.

Control algorithm

At the beginning of each trial, the participant contacted the movable plate which was placed at the center of the testing apparatus. As the normal force of the fingertip on the plate exceeded the threshold value of <0.3 *N*, the plate position was updated every 5 *ms*, according to Equation 5:

$$\begin{bmatrix} x \\ y \end{bmatrix}_{new} = \begin{bmatrix} x \\ y \end{bmatrix}_{old} + \begin{bmatrix} \gamma_x & 0 \\ 0 & \gamma_y \end{bmatrix} \left(\begin{bmatrix} X \\ Y \end{bmatrix}_{new} - \begin{bmatrix} X \\ Y \end{bmatrix}_{old} \right) \quad \text{(Equation 5)}$$

Where x_{old} and x_{new} are the x position of the contact plate in the previous and in the current step, $(X_{new} - X_{old})$ is the displacement of the fingertip along that axis, and y_{old}, y_{new}, Y_{old}, Y_{new} are the corresponding variables along the y axis. The parameters γ_x and γ_y are arbitrary values of gain set by the experimenter that modify the relatioship between the displacement fingertip and the update of the contact plate along each axis. In each trial γ_x and γ_y were each set to one of three possible values (-0.7, 0 or 0.7), generating 9 possible x-y gain combinations. Negative gain means that the plate was moving opposite to the hand movement along the axis, and positive gain means that the plate was following it. Both $[X, Y]_{new}$ and $[X, Y]_{old}$ were initialized to the current finger position at trial onset.

In three experiments, we investigated the role of slip motion (gain) on the reaching movement, with and without visual feedback on hand displacement. In all experiments, the plate and the hand of the participant were hidden from participants' sight by a curtain and wooden panel. In the **second experiment**, a visual feedback of the finger motion path was displayed on the PC monitor. In experiments 1 and 2, the plate was lubricated with ultrasound gel prior to each experimental session, in order to reduce the shear force on the fingertip. In the **third experiment**, the plate was lubricated either with ultrasound gel or seed oil prior to each session.

The first experiment consisted of a training session and a testing session. Before the training session, the experimenter moved the hand of the participant over the plate to demonstrate the proper velocity of movement during the experiment. Then the training session started, which consisted of 20 trials. The testing session of 135 trials followed the training session. The experimental procedure in the testing session was the following: The participant sat on a stool placed in front of the apparatus which was adjusted according to the height of each participant. Ear plugs and pink noise delivered with earphones masked the noise of the haptic device. In each trial, participants were requested to contact the plate with their right index finger and two dots indicating the starting and the target position on the plate were displayed on the PC monitor (Figure 2B). Throughout trials, the target position was shown either 45° to the left or to the right of the starting position, or in front of it at 0°. Participants were instructed to slide their finger on the surface of the plate along a straight path towards the target. During the reaching movement, the position of the contact plate was updated according to Equation 1. The values of gain γ_x and γ_y changed pseudo-randomly across trials. The participant lifted the finger from the plate where they estimated that the target position had been reached. When the contact force was <0.3 *N*, the visual target disappeared and the plate changed color from black to red to alert the participant that the trial was over. After each trial, a warning signal was provided on the computer screen if the force exceeded the threshold value of 2 *N* or the length of the trajectory was more than 90 mm from the starting position. During the training session participants performed the same reaching task as in the testing session, with two important differences. The plate was not moving (i.e., $\gamma_x = 0$, and $\gamma_y = 0$). During the first 10 trials of the training we provided participants with a visual feedback, consisting of a blue dot indicating the position and motion of the finger on the plate. During the last 10 trials, only the starting position, target position, and the plate were displayed on the PC monitor, as in the testing session.

We ran a second experiment to disentangle the effects due to the mechanical perturbation from the moving plate and the functional effects due to the biased feedback. The control experiment was similar to the main experiment with the exception that a moving dot on the PC monitor provided visual feedback on finger position and motion, as in the first 10 training trials of the main experiment.

In a third experiment (experiment 3), we evaluated the role of tactile acuity and shear force in modulating the effects of gain observed in the first experiment. The two factors (i.e. tactile acuity and shear force) were manipulated using a factorial design, as follows. Across conditions, the plate was lubricated with two different lubricants: either ultrasound gel (used in two conditions: bare-fingertip and with thimble) or seed oil (used only in one bare-fingertip condition). As measured in previous studies, the friction coefficient of ultrasound gel is lower than the one of seed oil.[34,35] Therefore, the use of different lubricants is expected to result in a modulation of shear forces during the reaching movement. Participants performed the reaching task similar to the first experiment, either with a rigid thimble covering their fingertip, or with their bare fingertip. In accordance with previous literature, exploring a surface while wearing a thimble or a glove reduces tactile acuity.[10,33,58]

The three blocks in Experiment 3 were labelled as follows: *gel* (bare-fingertip with gel lubricant), *oil* (bare-fingertip with oil lubricant), and *thimble* (fingertip covered by thimble with gel lubricant), respectively. Their order was randomized across participants using a Latin square design. As in the first experiment, participants received no visual feedback about the movement and position of the hand during the reaching movement. To reduce the duration of the experiment and prevent fatigue, only a subset of the conditions used in Experiment 1 and 2 were tested in Experiment 3. Namely, each block consisted of only two targets (the left and the right targets) and four gain conditions (the combination of ± 0.7 along the x axis and ± 0.7 along the y axis). This design resulted in a total of 168 trials performed by each participant and divided into the three blocks (56 trials per block). Before each block, participants practiced with the task in a short training section (20 trials, as in experiment 1 and 2).

In addition, we conducted a rating test to evaluate the tactile acuity associated with the three conditions of Experiment 3. We instructed a group of participants (n = 10) to explore the surface of the device with a back and forth movement of the hand for several seconds. After they explored all three conditions, they were inquired about tactile acuity associated with each of them ("how easy is to perceive the fine texture of the surface?") and were requested to order the conditions from the most difficult to the easiest to discriminate. Then, they rated the tactile acuity in each condition on a Likert scale from 1 (dull sensation) to 7 (sharp sensation).

QUANTIFICATION AND STATISTICAL ANALYSIS

We evaluated the effect of x and y gain on the reaching movement. We analyzed the following parameters of the hand movement: velocity, motion path, and contact force. The analyses explained below were performed separately for the three experiments, with and without visual feedback. In each frame, the velocity along the x and the y axis was computed as difference between the initial and the final position divided by the duration of the frame (5 ms). Position, velocity, and force signal were filtered with a Butterworth 5^{th} order filter (cut-off frequency 10 Hz). In each trial and for each participant, we saved the final position, the peak value of velocity, and the peak value of force (tangential and normal force) of the filtered signals. Outliers (velocity peak exceeding 3 standard deviations from the mean, total trial time less than 1 s) were removed from analysis. Linear mixed models (LMM; function **lmer()** from the R package **lme4**) were used that account separately for random effects variability (between participants) and residual variability. Default diagnostic plots from package lme4 were used to ensure that the residuals of the models met the assumption of this statistical approach. We tested the predictions discussed in paragraph "Model and Predictions". First, by means of LMMs, we tested the hypothesis of a linear relationship between the motion velocity and the gain values (Figure 3D). For the central target, the speed along the x axis is expected to be zero and therefore should not be affected by the x gain. By means of LMM, we tested the hypothesis that, for each axis of motion, the path length is a linear function of the related value of gain along that axis (Figure 3C). Along the x axis, the slope of the linear relationship is either negative, zero, or positive depending on the target. Instead, along the y axis the model predicted an always positive linear relationship. Finally, we tested the prediction of the model that the cotangent of the motion angle—computed as the ratio of the x and y thimble position at the end of the trial—is a nonlinear function of the cotangent of the target angle $\cot(\bar{\theta})$ and of the two gain values γ_y and γ_x, with w_c being the single free parameter of the model:

$$\cot(\theta) = \cot(\bar{\theta})\frac{1 - w_c\gamma_y}{1 - w_c\gamma_x} \quad \text{(Equation 6)}$$

Nonlinear least squares model (function **nls()** from the R package **stats**) was used to fit the nonlinear equation to the data. For a given pair γ_y, γ_x, this reduces to the linear model in Equation 3, with

$$\beta\left(w_c, \gamma_y, \gamma_x\right) = \frac{1 - w_c\gamma_y}{1 - w_c\gamma_x} \quad \text{(Equation 7)}$$

The statistical analysis was performed in R version 4.1.0. Signal filtering was implemented in Python version 3.9.2 (function **filtfilt()** from Python package Scipy).

Predictions of the vector model

Figure 3 of the manuscript illustrates the predictions of the vector model detailed below. We used the following notation: the letter h, p, and s indicate the velocity of the hand, the velocity of the plate, and the velocity of slip motion, respectively. The subscript indicates either the x or y velocity component. For simplicity, we used the subscript i when the same equation refers to the two axes of motion. The estimated velocity is indicated with a hat sign, for example, $\widehat{p}$ is the hand velocity as measured from the observer. The desired velocity is indicated with a vertical bar, for example $\overline{p}$. For each axis of motion, the velocity of slip motion is the difference between the plate and the actual hand velocity:

$$s_i = p_i - h_i$$

Because of to the control algorithm of the apparatus, the velocity of the plate is:

$$\frac{dP}{dt} = \gamma_i \frac{dH}{dt} = \gamma h_i$$

where $P = x(t+1) - x(t)$ and $H = X(t+1) - X(t)$ are the displacement of the plate and the hand between two intervals, respectively. The gain γ_i was set by the experimenter for each trial. Therefore,

$$s_i = \gamma_i h_i - h_i = h_i(\gamma_i - 1)$$

To simulate the response of the ideal observer, we assumed that the duration of the reaching movement $t = 1$ seconds, corresponding to a desired hand speed $\overline{h} = 60$ mm/s (with the target distance equal to 60 mm). The measured velocity of the hand $\widehat{h}_i$ was a weighted sum of proprioception and touch. For each axis of motion i in the x-y plane:

$$\widehat{h}_i = w_k \widehat{h}_{ik} + w_c \widehat{h}_{ic}$$

with $w_k + w_c = 1$. The velocity estimate from proprioception was unbiased and equal to the actual hand velocity. For each of the two motion axes:

$$\widehat{h}_{ik} = h_i + \epsilon_{ik}$$

Because of the *static prior*, the slip velocity provided an auxiliary cue of hand velocity. We referred to this as the cutaneous estimate of hand velocity:

$$\widehat{h}_{ic} = -s_i + \epsilon_{ic}$$

Therefore, we can substitute in the first equation

$$\widehat{h}_i = h_i w_k - h_i(\gamma_i - 1)w_c = h_i[w_k - w_c(\gamma_i - 1)] = h_i(1 - w_c\gamma_i)$$

with the two velocity components being equal to:

$$\begin{bmatrix} \widehat{h}_x \\ \widehat{h}_y \end{bmatrix} = \begin{bmatrix} (1 - w_c\gamma_x)h\,cos(\theta) \\ (1 - w_c\gamma_y)h\,sin(\theta) \end{bmatrix}$$

The model predicts that participant adjusted the x- and y-component of the hand velocity to match the desired motion angle $\overline{\theta}$. That is, they corrected their movement according to the equation below:

$$\tan(\overline{\theta}) = \tan(\widehat{\theta}) = \frac{\widehat{h}_y}{\widehat{h}_x} = \frac{(1 - w_c\gamma_y)h\,sin(\theta)}{(1 - w_c\gamma_x)h\,cos(\theta)} = \tan(\theta)\frac{(1 - w_c\gamma_y)}{(1 - w_c\gamma_x)}$$

Therefore, the actual motion angle θ (for $\overline{\theta} \neq \pi/2$) was:

$$\theta = \arctan\left(\tan(\overline{\theta})\frac{1 - w_c\gamma_x}{1 - w_c\gamma_y}\right)$$

The x component of the hand velocity was:

$$h_x = h\,cos(\theta) = \frac{\widehat{h}_x}{1 - w_c\gamma_x}$$

Since we assumed that after movement correction the perceived velocity component was equal to the desired velocity component $\widehat{h}_x = \overline{h}_x = \overline{h}cos(\overline{\theta})$, then:

$$h_x = \frac{\overline{h}cos(\overline{\theta})}{1 - w_c\gamma_x} = \frac{60\,cos(\overline{\theta})}{1 - w_c\gamma_x}$$

where $\overline{\theta}$ is the stimulus angle and $|\overline{h}|$ = 60 mm/s (as we assumed motion duration to be 1 second). Likewise, the y component was:

$$h_y = \frac{60 \sin(\overline{\theta})}{1 - w_c \gamma_y}$$

The hand velocity can be computed as

$$h^2 = h_x^2 + h_y^2$$

Finally, the path length can be predicted by multiplying the actual velocity h times the motion duration that we assumed to be constant and equal to 1 second.